Nicotinamide and Picolinamide in Phospholipid Monolayers

María Florencia Martini,[a,b] Edgardo Aníbal Disalvo,[b] and Mónica Pickholz[a,b]

Molecular dynamics simulations have been performed to investigate the interactions between nicotinamide (NA) and picolinamide (PA) with Langmuir monolayers of zwitterionic lipids: dimyristoylphosphatidylcholine (DMPC) and dimyristoylphosphatidylethanolamine (DMPE). Our results for the DMPC monolayers show that both NA and PA molecules are essentially found at the lipid/water interface and present orientational disorder of the molecules. In the case of DMPE monolayers, the pyridine nitrogen seems to be located deeper inside the monolayer than the amide group, for both isomers, being the effect higher for PA. We have computed electrostatic surface potentials and found qualitatively good agreement with experimental results. The different orientation and specific interactions of each molecule determine changes in the head orientation of the phospholipids, as the case of PA in DMPE monolayers, or in the orientation of the water dipoles, as it is the case of PA in DMPC monolayers. Through these analyses, we were able to capture the main contributions to the electrostatic potential in each system.

DOI: 10.1002/qua.24124

Introduction

Nicotinamide (3-pyridinecarboxamide, niacinamide, Vitamin B3, NA) and picolinamide (2-pyridinecarboxamide, PA) (Fig. 1) show important biological activity with a coenzyme called nicotinamide adenine dinucleotide.[1] This coenzyme plays important roles in more than 200 amino acid and carbohydrate metabolic reactions.[2] The two regioisomers of pyridine-carboxamide are a class of medicinal agents with activity that includes the reduction of iron-induced renal damage,[3] the treatment of diabetes type 1,[2] pellagra,[4] and radio/chemosensitization.[5]

The elucidation at the molecular level of the interactions of bioactive species with phospholipid constituents of biological membranes has a fundamental importance to understand their mechanisms of action. The interaction of bioactive molecules with biomembranes depends on their nature (more polar molecules interact essentially with the lipid heads while hydrophobic molecules penetrate deeper into de lipid tail region).[6,7] As NA and PA are hydrophilic molecules, a way to get an insight on their interaction with lipids is to study the effects on the membranes when bioactive species bind to groups that remain exposed to water. These groups are preferentially carbonyls in the glycero-acyl ester union and phosphates in the phospholipids head groups.[8]

Experimental evidences showed that the interaction of NA and PA with lipid membranes depend on the type of lipid head groups. Based on dipolar potential results on lipid monolayers, Borba et al.[9] suggest a stronger interaction of NA molecules with lipids bearing phosphatidylcholine (PC) other than phosphatidylethanolamine (PE) head groups. Furthermore, these authors found no significant difference in the interaction of PA with both types of lipids.

Despite many advances in the study of lipid monolayers/bilayers, there exists an intrinsic limitation in the interpretation of experimental results, which is generally based on continuum theories. Thus, many important features of these systems—at molecular level—become hardly accessible. In that sense, atomistic simulations provide a powerful tool for studying the interactions of small molecules with phospholipid monolayers, allowing explore—in a nanoscopic detail—statistical mechanical properties, structure, and dynamics of these systems, establishing a close connection with experimental data.[10]

In an attempt to explain the results in atomistic scale, Borba et al.[9] carried out quantum chemistry calculations on the interactions of NA and PA with a single lipid. Through these calculations, they identified key specific interactions between nitrogen compounds and a single lipid molecule. It should be noted that these models do not take into account collective effects or lipid packaging, which are fundamental to understand this kind of systems.

To make some progress in this direction, we use molecular dynamics (MD) simulations to study the interaction of NA and PA with dimyristoylphosphatidylcholine (DMPC) and dimyristoylphosphatidylethanolamine (DMPE). Through these simulations, we aim to answer several questions that remain open about these systems. For example: location and orientation of PA and NA in the monolayer, lipid tails organization in the presence of the compounds, lipid head groups orientation, and specific interactions between bioactive lipids, among others.

[a] *M. Florencia Martini, M. Pickholz*
Department of Pharmaceutical Technology, Faculty of Biochemistry and Pharmacy, University of Buenos Aires, C.P. 1113, Buenos Aires, Argentina
[b] *M. Florencia Martini, E. A. Disalvo, M. Pickholz*
CONICET, Buenos Aires, Argentina

Contract grant sponsor: Agencia Nacional de Promoción Científica y Técnica; Contract grant number: PICT 2008/310.
Contract grant sponsor: UBACyT; Contract grant number: 20020090200384.
Contract grant sponsor: CONICET; Contract grant number: PIP 11220100100401.

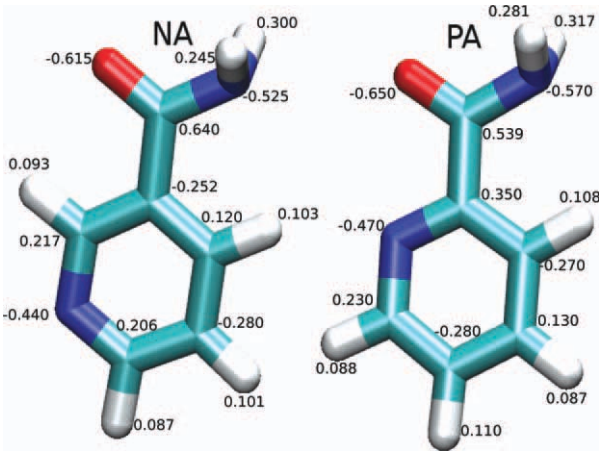

Figure 1. Molecular structure of NA and PA with the correspondent atomic charges. [Color figure can be viewed in the online issue, which is available at wileyonlinelibrary.com.]

In the next section, we describe the simulated systems and the computational details. The main results and concluding remarks are presented in Simulation Results and Concluding Remarks sections, respectively.

Methods and Computational Details

We have performed atomic-scale MD simulations of single-component lipid monolayers comprised of zwitterionic DMPC and DMPE lipids in aqueous solution of NA or PA in each case. The simulated systems, in the case of DMPC, consist of a periodically replicated cell containing 128 lipids, divided into two monolayers with 64 lipids each and 40 molecules of NA or PA, depending on the case. The monolayers are separated by a slab containing 8100 water molecules. The system is effectively periodic in 3D and no interactions are expected across the *z* direction (normal to the interfaces) because of the large vacuum region, as depicted in Figure 2. In the case of DMPE systems, the scheme is quite similar: a periodically replicated cell containing 132 lipids, divided into two monolayers with 66 lipids each and 40 molecules of NA or PA. The monolayers are separated by a slab containing 8500 water molecules. The simulation geometry is similar to that proposed by Feller et al.[5] and has been used in many studies.[11–14] The size of the simulation cell was kept constant. The in-plane box dimension, *Lx* and *Ly*, were chosen to accommodate the lipids on each interface at the appropriate area per lipid (62 Å^2 for DMPC and 60 Å^2 for DMPE monolayers[15–17]). The *Lz* was kept at 255 Å in all cases, to ensure that interactions across the *z* axis were negligible for each surface density considered.

In all the cases, the corresponding bioactive molecule concentration is ∼250 mM and the molecule:lipid ratio is ∼1:3, in agreement with the experimental information that we find in bibliography.[9] The same types of systems in the absence of NA or PA were performed as controls of the behavior of neat lipid monolayers.

The MD simulations were performed by GROMACS 4.0 software package.[18–20] The GROMOS-96 53a6 force field[21,22] was used for the four type of molecules (NA, PA, DMPC, and DMPE). Methylene and methyl groups of lipid molecules were treated as united atom type. Water was modeled using the simple point charge model.[23] The electrostatic interactions were handled with the smooth particle mesh ewald (SPME) version of the Ewald sums.[24,25] The settings for the SPME method were a real space cutoff of 1.5 nm, a grid spacing of 0.24 nm, and a cubic interpolation. In all the simulations, the van der Waals interactions were cutoff at 1.5 nm. The simulations were carried out in the NVT ensemble using the Berendsen thermostat.[26] The whole system was coupled to a temperature bath with a reference temperature of 300 K and a relaxation constant of 0.1 ps. No constraints were used for the bonds. The time step for the integration of the equation of motion was 1 fs. The nonbonded list was updated every 10 steps. To release steric clashes we performed 1,000,000 steepest descent cycles and 1,000,000 steps of conjugated gradient algorithm. Prior to the production run, a series of six equilibration steps of 5 ns each were performed upgrading the temperature progressively.

The ground-state geometry of NA and PA was optimized within the density functional theory with use of the B3LYP[27] functional and 6-31G* basis set. The molecular structure of these molecules is shown in Figure 1. The partial atomic charges were obtained through a single point HF/6-31G*using Gaussian[28] and the Merz–Singh–Kollman protocol.[29] The force constants and intermolecular parameters were chosen in analogy to similar molecules already described by GROMOS.

The simulated systems were built in a cubic box, using the Packmol package[30] sampling the bioactive molecules near the

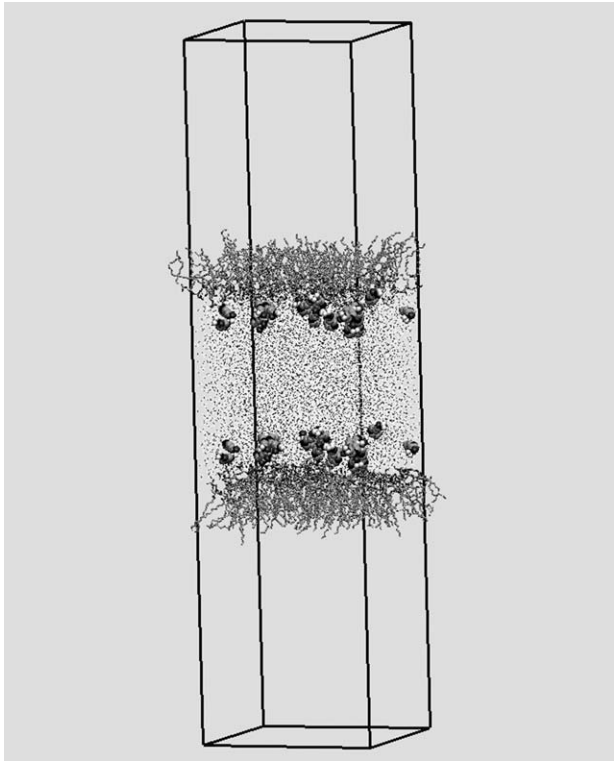

Figure 2. Scheme of the simulation unit cell on the beginning of the simulation.

monolayers, but not inside them (e.g., see Fig. 2). The system's dimensions were carefully chosen to ensure an aqueous layer of at least 50 Å between the headgroups of the two opposing monolayers, therefore ensuring negligible interactions between lipid surfaces[5]. MD simulations were carried out up to 100 ns production run after the equilibration of the system. The images were made with visual molecular dynamics (VMD)[31] and Grace (xmgrace)[32] software.

Simulation Results

Electron density profiles

The interfacial ordering of the system is evaluated here by means of the electron density profile (EDP) normal to the monolayer. The profiles were calculated by time averaging the net charge per 0.1 Å thick slabs, assuming a Gaussian distribution centered at the atomic positions with a width of approximately 2 Å. Figure 3 shows EDPs for the six systems under investigation, with the electron density being plotted against the z coordinate, where $z = 0$ corresponds to the system center

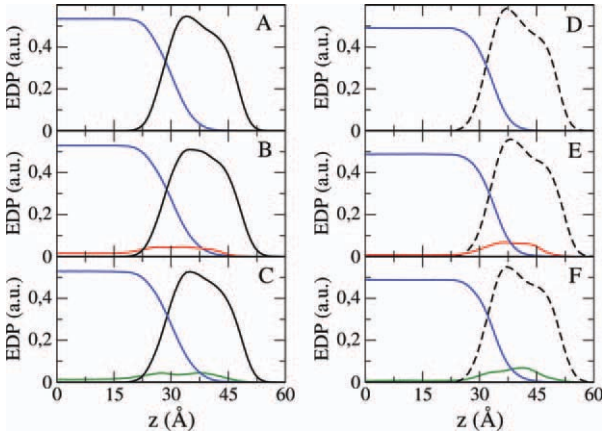

Figure 3. EDP of the main system constituents: water (dotted lines), NA (dot-dash-dashed lines; amplified two times for comparison propose), PA (dash-dot-dotted lines; amplified two times for comparison propose), the monolayers of DMPC (black solid lines), and DMPE (black dashed lines). (A) Neat DMPC; (B) NA in DMPC monolayers; (C) PA in DMPC monolayers; (D) neat DMPE; (E) NA in DMPE monolayers; and (F) PA in DMPE monolayers.

located in the middle of the aqueous phase. Contributions to the electron density are shown for water, NA, or PA (both molecules were amplified by a factor 2 for comparison purposes) and for monolayers of DMPC or DMPE, depending on the case.

A comparison of the profiles in panels (A) through (C) indicates that in the case of DMPC monolayer both bioactive molecules are predominantly found in the region of the polar head groups of the monolayers. On the other hand, in the case of DMPE monolayer (panels (D) through (F)), the molecules enter deeper into the hydrophobic core of the monolayer tails. This effect is more pronounced for the case of PA molecules (dash-dot-dotted lines).

Further details about NA and PA orientation can be obtained by analyzing the distribution of its main groups,

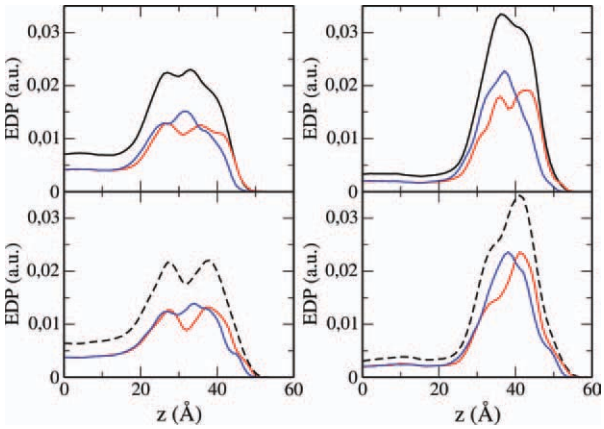

Figure 4. Total and partial contributions to EDPs of NA and PA in DMPC (left) and DMPE (right) monolayers. The total EDP of NA is shown in black solid lines, PA in black dashed lines, the N of the pyridine ring and N of the amide group contributions are depicted in gray and dot-dashed solid lines, respectively. Both partial contributions were amplified five times for comparison proposes.

depicted in Figure 4 for NA (top panels) and PA (bottom panels) molecules. The left panels represent the molecules in the DMPC monolayer, while the right panels represent the molecules in the DMPE monolayer. Separate group contributions to the EDPs are given for the nitrogen of the pyridine ring structure (gray solid lines) and the nitrogen of the amide group (dot-dashed lines). The overall lineshape of the distribution (not the mean location) of NA and PA appears to be affected by the monolayer composition, DMPC or DMPE. In the case of DMPC monolayers, both types of molecules present a broad distribution for both ring and amide nitrogen atoms, with distribution maxima near each other suggesting an orientational disorder of the molecule. In contrast, in DMPE monolayers, the pyridine nitrogen seems to be deeper inside the monolayer than the amide group. Mainly PA shows a different preferential region for each group: the ring makes deeper incursions into the hydrocarbon core than does the amide group, suggesting that specific interactions between this last group and the polar head groups of DMPE may be taking place.

Specific interactions

To get deeper insights on the possible orientation of the different molecules in the lipid monolayer, we study the specific interactions between the principal donors and acceptors of hydrogen bonding groups. Figure 5A shows the radial distribution function, $g(r)$, between the oxygens of phosphate group and the hydrogens of the amide group of NA (gray) and PA (black) with DMPC (solid lines) and DMPE (dashed lines), respectively. The first peak, for the four cases, located at ~1.98 Å, is characteristic of a hydrogen (H)-bonding.[33] It is more pronounced in DMPE for both molecules. Besides, PA molecules show stronger interactions between these groups than NA with both kinds of lipids.

Figure 5B shows, using the same colors and type of lines than in Figure 5A, the $g(r)$ between carbonylic oxygens of the phospholipids and hydrogens of the amide group of the

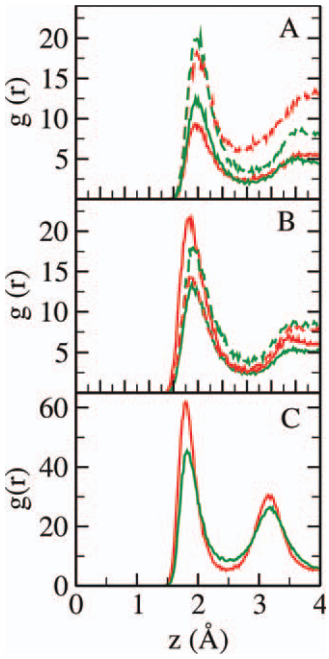

Figure 5. Radial distribution function between: (A) the hydrogens of the amine groups of NA (gray) and PA (black) and the phosphate oxygens for DMPC (solid lines) and DMPE (dashed lines), (B) carbonilic oxygens of DMPC (solid lines) and DMPE (dashed lines) and hydrogens of the amide group of NA (gray) and PA (black), (C) amide oxygen group of NA (gray) or PA (black) and the hydrogens of the ethanolamine group of DMPE.

molecules. Again, the first peak for the four cases located at ~1.85 Å, suggesting the existence of an (H)-bonding. In this case, the peak is more pronounced for NA in DMPC monolayers, as we discuss in terms of the EDPs (Fig. 4), where a maxima in the middle of the interfacial region was found. This result suggests a pivotal position of NA with the amide group interacting with the carbonyl and two possible orientations to the pyridine ring, pointing to the monolayer interior or to the aqueous region, respectively.

In Figure 5C, we evaluate the interaction of the amide oxygen group of NA or PA and the hydrogens of the ethanolamine group. This kind of interaction is possible only in the case of DMPE, because the choline group present methylenes instead of hydrogens. A sharp peak in ~1.80 Å corresponds again to a specific interaction between these two groups. The fact that this interaction is stronger for NA is in good agreement with a preferential location of this molecule (closer to the aqueous phase in the monolayer). The distribution of the different polar groups in the interphase of DMPE is, essentially, going from aqueous region to hydrocarbon tails: ethanolamine, phosphate, and carbonyls groups (data not shown). In this sense, a higher interaction of NA with hydrogens of ethanolamine group suggests a preference position closer to the aqueous phase than PA.

Lipid tail ordering

The lipid tail order parameter is a standard quantity to evaluate the structural order of acyl chains in lipid bilayers, which can be obtained from deuterium NMR measurements. The experimental order parameter, $S_{CD} = -1/2S_{mol}$, is derived from the measured residual quadrupole splitting $\Delta\nu = (3/4)(e^2qQ/h)$ S_{CD}.[34] In MD simulations, it can be determined by:

$$S_{mol} = \frac{1}{2}\langle 3\cos^2\theta_n - 1\rangle,$$

where θ_n is the angle between the normal to the bilayer and the normal to the plane defined by two carbon—deuterium (C—D) bonds in a deuterated *n*-methylene group of the lipid acyl chain. If a united atom forcefield is used (without hydrogen or deuterium atoms), the C—D bond vector needs to be reconstructed. In this way, the C(i – 1) – C(i + 1) vector is usually taken to be the *z*-axis. The *x*- and *y*-axis are defined perpendicular to the *z*-axis and to each other, with the *y*-axis in the C(i – 1) – C(i) – C(i + 1) plane. Using this definition, $S = (2/3)Sxx + (1/3)Syy$ and can be compared directly to ^{2}H NMR data.[35,36]

The order parameter is related to the tilt angle of the chains and to trans-gauche distribution of chain dihedrals, but the relationship is indirect.[11(a)] Figure 6 shows the -S_{CD} order

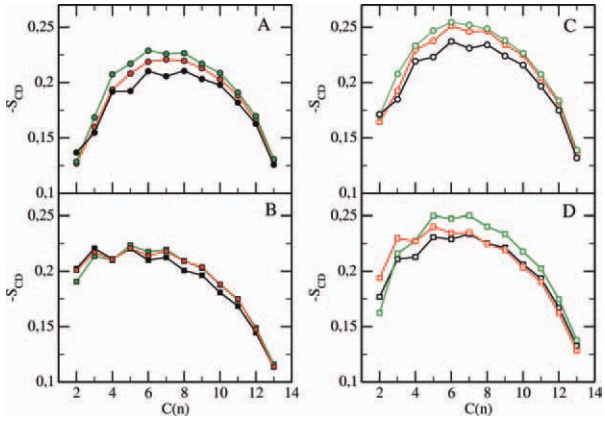

Figure 6. Order parameters (-S_{CD}) as a function of the position of the carbon atoms along the hydrocarbon chain of DMPC sn-1 (A), sn-2 (B) and DMPE sn-1 (C), sn-2 (D). Neat (solid lines), with NA (dashed lines) and with PA (dotted lines).

parameters for all lipid methylene groups for sn-1 and sn-2 DMPC hydrocarbon tails (in order: panels A and B) and the same for DMPE (panels C and D), with and without NA or PA. The CH_2 groups are numbered consecutively from 2 to 13. The carbonyl and CH3 carbons are labeled 1 and 14, respectively. Overall, the results are typical of phospholipid monolayers showing higher orientational order (larger -S_{CD}) for the methylene groups located in the middle of the lipid tails.

PA introduces important changes in the tail ordering. The effects are significantly more noticeable in DMPE monolayers. This is consistent with PA entering deeper in this type of monolayer, thus contributing to a reduction of the effective surface area per lipid.[20,37] By the other hand, the presence of the NA molecules also promotes ordering effect

on the monolayers; however, their effect is weaker than PA case.

Electrostatic potential across the interface

The electrostatic potential (ψ) across the interface, arising from the nonuniform distribution of dipoles, can be computed from a trajectory by evaluating the double integral of the charge density $\rho(z)$:

$$\psi(z) - \psi(-\infty) = -\int_{-\infty}^{z} dz' \int_{-\infty}^{z'} \rho(z'')dz''/\varepsilon_0$$

where the position $z = -\infty$ is far enough in the bulk phase that the field is zero, and $\rho(z)$ is the time averaged charge. The double integral of the charge density gives the electrostatic potential.

The results are shown in Figure 7, where the potential at the air region has been set to zero. For a pure DMPC mono-

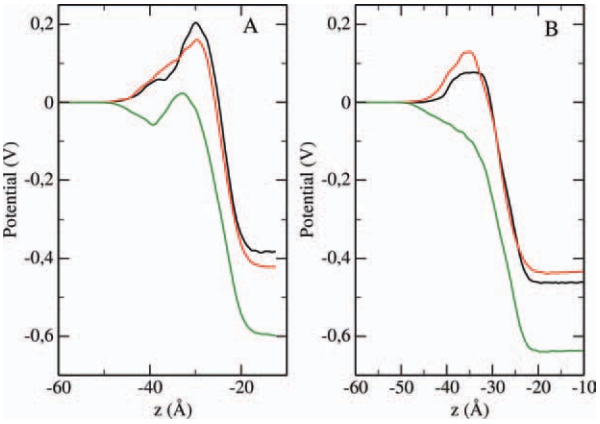

Figure 7. Electrostatic potential for DMPC (panel A) and DMPE (panel B), for neat (solid lines), with NA (dashed lines) and PA (dotted lines).

layer (panel A, black solid line), we obtain −386 mV, which is in agreement with previous MD simulation studies.[38–40] Experimental data for phospholipid membranes range from −200 to −600 mV.[41–47]

As we can see in Figure 7, the changes due to the presence of PA (dotted lines) are ∼200 mV in DMPC and ∼176 mV in DMPE monolayers. These results are in very good agreement with the changes on the dipole potential obtained experimentally for Borba et al.[10]. These authors obtained changes of ∼200 mV for PA in both types of lipids, at the same concentration of bioactive molecule.

The results show that NA effects on the electrostatic potential are weaker than the PA ones for both types of lipids. We obtain changes of ∼45 mV in DMPC and ∼30 mV in DMPE. This is in good qualitatively, with the experimental results (where values of ∼100 and 40 mV are reported for DMPC and DMPE, respectively).[10]

It is important to remark that the electrostatic potential arise from the nonuniform distribution of dipoles. In this way, dipole contributions, in these systems, arise from the orientations of the lipid heads, of the guest molecules and the distribution of water dipoles toward the interphase. In many cases, dipoles of the different groups are cancelled, showing no neat effect in the electrostatic potential.

To exploit the possibilities that offer the computer simulations, in next subsections we look at the changes of the lipid heads and their contributions to the electrostatic potential. Considering that one of the main dipole contributions to the potential is the $\mathbf{P}^- \rightarrow \mathbf{N}^+$ vector, we study its contribution for the different systems.

Analysis of the headgroups

The effects from NA and PA on the lipid headgroups of the monolayers can be analyzed in more detail by inspecting the orientation probability distribution of the charged groups **P** and **N** of the zwitterionic lipid heads. Let θ as the angle between the $\mathbf{P}^- \rightarrow \mathbf{N}^+$ vector and the monolayer normal vector. An angle of 0° corresponds to a vector aligned with the axis of reference pointing toward the aqueous phase, and an angle of 180° corresponds to a vector pointing toward the monolayer hydrocarbon tails.[48] The orientation probability distributions, $\mathbf{P}(\theta)/\mathbf{P}^{iso}(\theta)$, calculated by averaging over all lipids and all configurations are depicted in Figure 8 for each type of

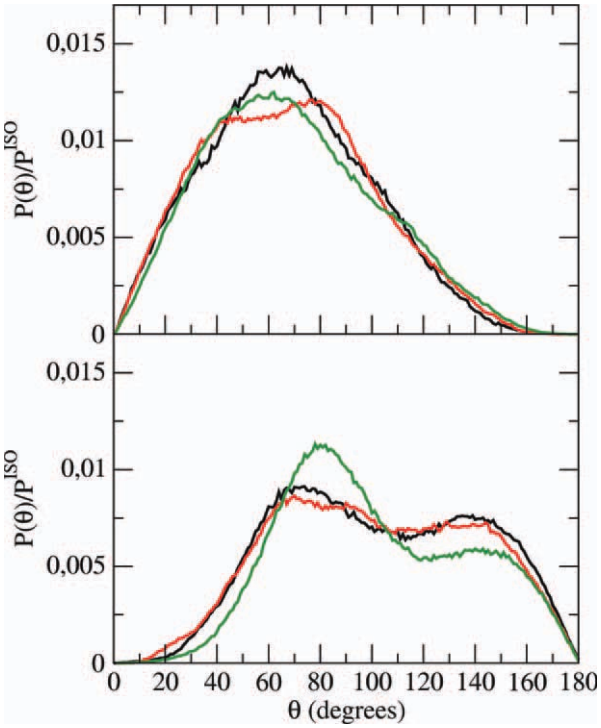

Figure 8. Orientational distribution, $\mathbf{P}(\theta)/\mathbf{P}^{iso}(\theta)$, of the θ angle between the headgroup **PN** vector and the bilayer normal for DMPC (top panel) and DMPE (bottom panel) monolayers. Neat (solid lines), with NA (dashed lines) and with PA (dotted lines).

lipid. In the case of DMPC the preferential orientation is around θ ∼65°, and the interaction with the bioactive molecules do not change significantly this situation. On the other

hand, the DMPE headgroup present two populations of angles in ~70° and ~140°. This is in good agreement with the capability of PE to form intermolecular (H)-bonding. Thus, there are two preferential orientations of the amine group: one near the interface (distribution <90°) and one near the lipid oxygen atoms of the phosphate groups indicating that the amine groups are favorably interacting with them (distribution >90°).[48] The interaction with NA does not modify this pattern. However, the interaction with PA changes the proportion of the populations significantly and shifts the population of 70–80°. The population angle of 140° shows a remarkable decrease in the presence of PA, suggesting a decrease in the intermolecular (H)-bonding of DMPE, in good agreement with the higher affinity of PA to the phosphate group of this lipid (Fig. 5). This change considerably affects the electrostatic potential of the monolayer (Fig. 7). In this sense, the change in the overall lineshape of PA interacting with DMPE is not only due to the PA itself but also due to the reorientation of the DMPE headgroups.

The changes in the electrostatic potential of DMPE due to the presence of NA and PA guest molecules should be understood due to the difference in the orientation of the PN vector and the water dipoles reorientation following this change. However, the picture is completely different in the DMPC where no noticeable changes were found in the PN vector orientation. Considering the contributions of dipoles to the electrostatic potential, water dipoles play an important role in that sense. It seems to be appropriate a discussion in this direction.

Water dipoles distribution

We computed the orientation of water molecules with respect to the vector normal to the monolayer, and we determined the average cosine of the angle between the dipole moment of water and the *z* axis.[46] The box is divided in slices and the average orientation per slice is printed. Each water molecule is assigned to a slice, per time frame, based on the position of the oxygen.

As we can see from Figure 9, the average direction of the water dipoles in the neat DMPC (solid line) monolayer–water interface region changes considerably in its interaction with PA (dotted line). This change is related with the "hump" effect close to the interface, which is due to a subtle imbalance between the orientation of the water molecules and lipid headgroups.[46] This effect does not occur in the case of NA (dashed line) interacting with DMPC. Therefore, the changes in the electrostatic potential in the case of DMPC monolayers would be explained because of a change in the water dipoles orientation, instead of a predominantly effect of a reorientation of the lipid headgroups as it is the case in DMPE.

Concluding Remarks

MD simulations were used to investigate the effects of the interaction of biomolecules as NA and PA on its location, relative orientation, and distribution and effects in zwitterionic DMPC and DMPE monolayers.

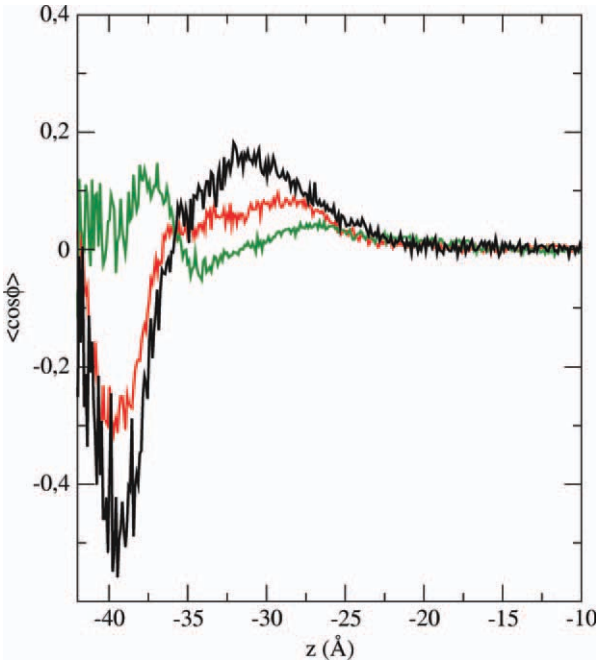

Figure 9. Projection of the water dipole unit vector $\vec{\mu}$ onto the interfacial normal $\rightarrow$, yielding $P(z) \equiv \langle \vec{\mu}(z) \cdot \rightarrow \rangle = \langle \cos\phi \rangle$ for neat DMPC (solid line), DMPC-NA (dashed line), and DMPC-PA (dotted line).

We can determine a distinct orientation of the molecules, mainly determined by the type of lipid composition of the monolayers. Both isomers present considerable specific interactions with the phosphate and the amine groups of DMPE. In the case of DMPC monolayers, NA presents an important specific interaction with the carbonyl oxygens.

The different orientation and specific interactions of each molecule determine changes in the PN vector of the phospholipids, as the case of PA in DMPE monolayers, or in the orientation of the water dipoles, as it is the case of PA in DMPC monolayers. This effects impact in the electrostatic potential of the system and modify it.

Acknowledgments

M.F.M., E.A.D, and M.P. are members of the Research Career from Consejo Nacional de Investigaciones Científicas y Técnicas (R. Argentina).

Keywords: molecular dynamics · picolinamide · nicotinamide · lipid monolayers

How to cite this article: M. Florencia Martini, EA. Disalvo, M. Pickholz, *Int. J. Quantum Chem.* **2012,** DOI: 10.1002/qua.24124

[1] R. A. Olsen, L. Liu, N. Ghaderi, A. Johns, M. E. Hatcher, L. J. Mueller, *J. Am. Chem. Soc.* **2003**, *125,* 10125.
[2] Dietary Reference Intakes for Thiamin, Riboflavin, Niacin, Vitamin B6, Folate, Vitamin B12, Pantothenic Acid, Biotin, and Choline, Institute of

Medicine; National Academy Press: Washington, DC, **1998**; pp. 123–149.
[3] T. Kawabata, T. Ogino, M. Mori, M. Awai, *Acta Pathol. Jpn.* **1992**, *42,* 469.
[4] Y. K. Park, C. T. Sempos, C. N. Barton, J. E. Vanderveen, E. A. Yetley, *Am. J. Public Health* **2000**, *90,* 727.
[5] (a) S. E. Feller, Y. Zhang, R. W. Pastor, *J. Chem. Phys.* **1995**, *103,* 10267; (b) S. E. Feller, Y. Zhang, R. W. Pastor, R. B. Brooks, *J. Chem. Phys.* **1995**, *103,* 4613.
[6] W. Caetano, M. Ferreira, M. Tabak, M. I. M. Sanchez, O. N. Oliveira, P. Kruger, M. Schalke, M. Losche, *Biophys. Chem.* **2001**, *91,* 21.
[7] S. H. White, *J. Gen. Physiol.* **2007**, *129,* 363.
[8] E. A. Disalvo, F. Lairion, F. Martini, E. Tymczyszyn, M. Frias, H. Almaleck, G. J. Gordillo, *Biochim. Biophys. Acta* **2008**, *1778,* 2655.
[9] A. Borba, F. Lairion, A. Disalvo, R. Fausto, *Biochim Biophys Acta* **2009**, *1788,* 2553.
[10] (a) L. Koubi, M. Tarek, M. L. Klein, D. Scharf, *Biophys. J.* **2000**, *78,* 800; (b) L. Koubi, L. Saiz, M. Tarek, M. L. Klein, D. Scharf, *J. Phys. Chem. B* **2003**, *107,* 14500; (c) Z. Liu, Y. Xu, P. Tang, *Biophys. J.* **2005**, *88,* 3784; (d) L. Koubi, M. Tarek, S. Bandyopadhyay, M. L. Klein, D. Scharf, *Biophys. J.* **2001**, *81,* 3339; (e) P. Tang, Y. Xu, *Proc. Natl. Acad. Sci. USA* **2002**, *99,* 16035; (f) L. M. Stimson, I. Vattulainen, T. Róg, M. Karttunen, *Cell. Mol. Biol. Lett.* **2005**, *10,* 563.
[11] S. O. Nielsen, C. F. Lopez, P. B. Moore, J. C. Shelley, M. L. Klein, *J. Phys. Chem. B* **2003**, *107,* 13911.
[12] Z. Li, B. Cranston, L. Zhao, P. Choi, *J. Phys. Chem. B* **2005**, *109,* 20929.
[13] A. F. de Moura, M. Trsic, *J. Phys. Chem. B* **2005**, *109,* 4032.
[14] M. Pickholz, O. N. Oliveira, Jr., M. S. Skaf, *J. Phys. Chem. B* **2006**, *110,* 8804.
[15] F. Lairion, E. A. Disalvo, *Biochim. Biophys. Acta Biomembr.* **2007**, *1768,* 450.
[16] F. Lairion, Universidad de Buenos Aires, PhD's dissertation, **2006**.
[17] R. P. Rand, N. Fuller, V. A. Parsegian, D. C. Rau, *Biochemistry* **1988**, *27,* 7711.
[18] H. J. C. Berendsen, D. van der Spoel, R. van Drunen, *Comput. Phys. Commun.* **1995**, *1–3,* 43.
[19] D. Van Der Spoel, E. Lindahl, B. Hess, G. Groenhof, A. E. Mark, H. J. C. Berendsen, *J. Comput. Chem.* **2005**, *16,* 1701.
[20] B. Hess, C. Kutzner, D. van der Spoel, E. Lindhal, *J. Chem. Theory Comput.* **2008**, *3,* 435.
[21] C. Oostenbrink, A. Villa, A. E. Mark, W. F. Van Gunsteren, *J. Comput. Chem.* **2004**, *13,* 1656.
[22] I. Chandrasekhar, M. Kastenholz, R. D. Lins, C. Oostenbrink, L. D. Schuler, D. P. Tieleman, W. F. van Gunsteren, *Eur. Biophys. J.* **2003**, *32,* 67.
[23] H. J. C. Berendsen, J. P. M. Postma, W. F. van Gunsteren, J. Hermans, In Intermolecular Forces; B. Pullman, Ed., Reidel: Dordrecht, **1981**, pp. 331–342.
[24] T. Darden, D. York, L. Pedersen, *J. Chem. Phys.* **1993**, *12,* 10089.
[25] U. Essmann, L. Perera, M. L. Berkowitz, T. Darden, H. Lee, L. G. Pedersen, *J. Chem. Phys.* **1995**, *19,* 8577.
[26] H. J. C. Berendsen, J. P. M. Postma, W. F. van Gunsteren, A. Dinola, J. R. Haak, *J. Chem. Phys.* **1984**, *8,* 3684.
[27] A. D. Becke, *J. Chem. Phys.* **1993**, *98,* 5648.
[28] M. J. Frisch, G. W. Trucks, H. B. Schlegel, G. E. Scuseria, M. A. Robb, J. R. Cheeseman, V. G. Zakrzewski, J. J. A Montgomery, R. E. Stratmann, J. C. Burant, S. Dapprich, J. M. Millam, A. D. Daniels, K. N. Kudin, M. C. Strain, O. Farkas, J. Tomasi, V. Barone, M. Cossi, R. Cammi, B. Mennucci, C. Pomelli, C. Adamo, S. Clifford, J. Ochterski, G. A. Petersson, P. Y. Ayala, Q. Cui, K. Morokuma, D. K. Malick, D. Rabuck, K. Raghavachari, J. B. Foresman, J. Cioslowski, J. V. Ortiz, B. B. Stefanov, G. Liu, A. Liashenko, P. Piskorz, I. Komaromi, R. Gomperts, R. L. Martin, D. J. Fox, T. Keith, M. A. Al-Laham, C. Y. Peng, A. Nanayakkara, C. Gonzalez, M. Challacombe, P. M. W. Gill, B. Johnson, W. Chen, M. W. Wong, J. L. Andres, C. Gonzalez, M. Head-Gordon, E. S. Replogle, J. A. Pople, GAUSSIAN98 (Revision A.7); Gaussian Inc.: Pittsburgh, PA, **1998**.
[29] (a) U. C. Singh, P. A. Kollman, *J. Comput. Chem.* **1984**, *5,* 129; (b) P. Cieplak, P. A. Kollman, *J. Comput. Chem.* **1991**, *12,* 1232.
[30] J. M. Martínez, L. Martínez, *J. Comput. Chem.* **2003**, *7,* 819.
[31] W. Humphrey, A. Dalke, K. Schulten, *J. Mol. Graphics* **1996**, *14,* 33.
[32] E. Stambulchik, Grace. 1998–2000 [retrieved June 20, 2009]. http://plasma-gate.weizmann.ac.il/Grace/.
[33] B. M. Ladanyi, M. S. Skaf, *Annu. Rev. Phys. Chem.* **1993**, *44,* 335.
[34] A. Seelig, J. Seelig, *J. Biochem.* **1974**, *13,* 4839.
[35] E. Egberts, S.-J. Marrink, H. J. C. Berendsen, *Eur. Biophys. J.* **1994**, *22,* 423.
[36] L. S. Vermeer, B. L. de Groot, V. Reat, A. Milon, J. Czaplicki, *Eur. Biophys. J.* **2007**, *36,* 919.
[37] M. Pickholz, O. N. Oliveira, Jr., M. S. Skaf, *Biophys. Chem.* **2007**, *125,* 425.
[38] S. W. Chiu, M. Clark, V. Balaji, S. Subramaniam, H. L. Scott, E. Jacobsson, *Biophys. J.* **1995**, *69,* 1230.
[39] R. R. Gabdoulline, G. Vanderkooi, C. Zheng, *J. Phys. Chem.* **1996**, *100,* 15942.
[40] A. M. Smondyrev, M. L. Berkowitz, *J. Chem. Phys.* **1999**, *111,* 9864.
[41] R. J. Clarke, *Adv. Colloid Interface Sci.* **2001**, *89,* 263.
[42] R. F. Flewelling, W. L. Hubbel, *Biophys. J.* **1986**, *49,* 541.
[43] K. Gawrisch, D. Ruston, J. Zimmerberg, V. A. Parsegian, R. P. Rand, N. Fuller, *Biophys. J.* **1992**, *61,* 1213.
[44] S. B. Hladky, D. A. Haydon, *Biochim. Biophys. Acta* **1973**, *318,* 464.
[45] A. D. Pickard, R. Benz, *J. Membr. Biol.* **1978**, *44,* 353.
[46] A. A. Gurtovenko, M. Patra, M. Karttunen, I. Vattulainen, *Biophys. J.* **2004**, *86,* 3461.
[47] M. del C. Luzardo, F. Amalfa, A. M. Nuñez, S. Díaz, A. C. Biondi de Lopez, E. A. Disalvo, *Biophys. J.* **2000**, *78,* 2452.
[48] S. Leekumjorn, A. K. Sum, *Biophys. J.* **2006**, *90,* 3951.

Received: 1 February 2012
Revised: 7 March 2012
Accepted: 12 March 2012
Published online on Wiley Online Library